Effect of double heterojunctions on the plasmon–phonon coupling in a GaAs/$Al_{0.24}Ga_{0.76}As$ quantum well



2008 Semicond. Sci. Technol. 23 125043

(http://iopscience.iop.org/0268-1242/23/12/125043)

IOP PUBLISHING SEMICONDUCTOR SCIENCE AND TECHNOLOGY

Semicond. Sci. Technol. **23** (2008) 125043 (5pp) doi:10.1088/0268-1242/23/12/125043

# Effect of double heterojunctions on the plasmon–phonon coupling in a $GaAs/Al_{0.24}Ga_{0.76}As$ quantum well

**H C Lee[1,4], K W Sun[2] and C P Lee[3]**

[1] Division of Electrical Engineering, National Space Organization, Hsinchu, Taiwan, Republic of China
[2] Department of Applied Chemistry, National Chiao Tung University, Hsinchu, Taiwan, Republic of China
[3] Department of Electronic Engineering, National Chiao Tung University, Hsinchu, Taiwan, Republic of China

E-mail: hanchiehlee@aa.nctu.edu.tw

Received 4 July 2008, in final form 13 October 2008
Published 21 November 2008
Online at stacks.iop.org/SST/23/125043

**Abstract**

Quasi-two-dimensional (Q2D) Coulomb interactions between plasmons and phonons in a GaAs quantum well are studied numerically. Based on the dielectric continuum model, the plasmon–confined phonon coupling and plasmon–symmetric (±) interface phonon coupling are considered. By using renormalized phonon propagators, six branches involving plasmon-like and phonon-like modes are obtained and used to study the effect on the hot-carrier average energy-loss rate (AELR). Plasmon-like modes are demonstrated to enhance the AELR around the sheet carrier density of $10^{11}$ $cm^{-2}$ due to a significant contribution of the plasmon–symmetric (+) interface phonon coupled mode. The importance of interface phonon modes on the plasmon–phonon coupling (PPC) is also indicated. If the interface phonon is not considered, the AELR enhancement due to the PPC will not appear. In addition, the carrier temperature is found to be important for the AELR enhancement. As the carrier temperature is as low as possible, the AELR enhances more remarkably because the effect of reabsorption of plasmon-like modes for hot carriers (hot-plasmon effect) can be greatly suppressed.

(Some figures in this article are in colour only in the electronic version)

## Introduction

Collective electronic oscillations in multiple quantum wells (MQWs) have shown an intrinsic difference from that in a bulk theoretically [1–7] and experimentally [8–12]. The broken spatial symmetry gives rise to several fundamental kinds of plasmons in MQWs. They can be categorized into intrawell (interwell) and intrasubband (intersubband) types when the Coulomb coupling between different layers and the quantum confinement are considered, respectively. Theoretically, the collective electronic oscillations, modeled by a large number electron in MQWs, were solved using the density matrix method within the self-consistent field approximation (SCF) [7]. The dispersion relations indicate that in the case of weak Coulomb coupling between adjacent quantum wells (QWs), the collective oscillation behaves like an ideal 2D electronic gas. At the long wavelength, the plasmon energy is proportional to the square root of the in-plane wave vector first proposed by Stern. In contrast, when the Coulomb coupling is strong, this would result in the optical and acoustic plasmon modes at the long wavelength, which are very similar to the lattice vibration in polar semiconductors. Otherwise, the intersubband plasmon is caused by the quantum confinement effect, which describes the collective electronic oscillation between different subbands in a QW. Many improved theories for intersubband plasmons have been developed [4–7]. The resonant screening (depolarization shift) [6], excitonic shifts (final-state correction) [7] and the vertex correction due to

[4] Address for correspondence: 9 F, 9 Prosperity 1st Road, 300 Hsinchu, Taiwan, Republic of China.

 

many-body effects [13] were taken into consideration to obtain a more accurate dispersion. By using the Raman spectroscopy, various types of plasmons have also been demonstrated experimentally [8–12]. The report of intrasubband and intersubband plasmons consisting a layered electron gas can be found in [9–11]. Systematic studies of intrawell and interwell plasmons in MQWs were reported in [12].

Since the electron gas is immersed in a crystal structure, the interaction between plasmons and phonons via the macroscopic electric field is unavoidable. In general, the so-called plasmon–phonon coupling (PPC) can be mathematically treated by using either electrodynamics or a many-body technique, as reported in [13, 14]. In the presence of double heterojunctions, the PPC behavior and its treatment become more complex and make it difficult to use both the above approaches unless we are guided by knowledge of given phonon and plasmon modes in a QW [15–20]. For instance, the intersubband plasmon between adjacent subbands would not couple to interface phonon modes because of their perpendicular polarizations. The previous one polarizes parallel to the crystal growth direction while another parallel to its propagation direction along heterointerfaces. Wendler and Pechstedt [20] attempted to obtain the PPC dispersions from the total dielectric function that accounted for the electron–electron, electron–interface phonon and electron–confined phonon interaction terms using the Dyson equation and the random phase approximation (RPA). Setting the real part of total dielectric function to zero, coupled dispersion branches can be obtained, showing a deviation from uncoupled plasmon and phonon branches.

In our report, the PPC in the presence of double heterojuctions was tackled by using the many-body technique. Differing from Wendler and Pechstedt [20], we assumed that intrasubband plasmons individually interact with confined and interface modes; that is, the plasmon–confined phonon coupling and the plasmon–interface phonon coupling are considered. Their dispersions can be obtained by using the renormalized phonon propagators, corrected by taking into account the effect of free electron gas [19]. The net plasmon–phonon generation rates can then be calculated and used to obtain the AELR. We found the scattering of plasmon-like modes considerable for the carrier relaxation around the sheet carrier density of $10^{11}$ cm$^{-2}$, where the AELR is enhanced due to the plasmon–interface phonon coupled mode. Meanwhile, the importance of the interface phonon on the PPC in a QW is also indicated. An anomalous result regarding the symmetric minus interface phonon is also presented. In addition, a striking dependence of the carrier temperature on the AELR enhancement is interpreted.

## Theory

In this section, the coupled dispersion relations and the net plasmon–phonon generation rates are presented. Based on the dielectric continuum model (DCM) [21–23], the symmetric plus (S+), the symmetric minus (S−) interface phonons and the confined (C) phonon were considered in a QW. Average phonon's energies of longitudinal (LO) and transverse optical (TO) modes in an AlGaAs layer [22] were assumed, with the material parameters taken from the report of Adachi [24]. Electrons in a QW were simplified by the ideal 2D electron gas and the plasma dispersion is given by [1]

$$\omega_p = \left(\frac{n_{2D}e^2}{2m_e\varepsilon_\infty}\mathrm{q}_{//}\right)^{1/2}, \tag{1}$$

where $n_{2D}$ is a sheet carrier density, $m_e$ is an electron's effective mass, $\varepsilon_\infty$ is a high-frequency dielectric constant and $\mathbf{q}_{//}$ is an in-plane wave vector.

Six PPC branches were considered. There are two of the plasmon–S+ interface (PS+), two of the plasmon–S− interface (PS−) and two of the plasmon–confined (PC) coupled modes. The renormalized phonon propagator due to the correction of free electron gas is given by [13]

$$D(\mathbf{q}_{//},\omega) = \frac{2\omega_i}{\omega^2-\omega_i^2-2\omega_i|M_i|^2\Pi_0(\mathbf{q}_{//},\omega)/\varepsilon(\mathbf{q}_{//},\omega)}, \tag{2}$$

where $\omega$ denotes the modified energy while $\omega_i$ represents the uncoupled phonon energy where the index $i$ denotes the S+, the S− and the C phonon modes. $M_i^2$ denotes the electron–phonon interaction strength and its expression was reported in [23]. The polarizability function $\Pi_0(\mathbf{q}_{//},\omega)$ and the dielectric function $\varepsilon(\mathbf{q}_{//},\omega)$ in the renormalized phonon propagator were adapted from [19], where the plasmon-pole approximation for the dielectric function was assumed and the Kramers–Kronig relation was used. The coupled dispersion relations and the coupled interaction strengths with electrons can then be given by [19]

$$\omega_{i(\pm)} = \sqrt{\frac{1}{2}\left\{\omega_i^2+\tilde{\omega}_p^2 \pm \left[\left(\omega_i^2-\tilde{\omega}_p^2\right)^2+8\omega_i\omega_p^2\frac{M_i^2}{\hbar V_{\mathbf{q}_{//}}}\right]^{1/2}\right\}}, \tag{3}$$

$$M_{i(\pm)}^2 = \frac{\omega_i}{\omega_{i(\pm)}}\frac{\left|\omega_{i(\pm)}^2-\tilde{\omega}_p^2\right|}{\omega_{i(+)}^2-\omega_{i(-)}^2}M_i^2 = C(\pm)M_i^2, \tag{4}$$

where $\omega_{\mathrm{i}(\pm)}$ $\left(M_{i(\pm)}^2\right)$ represents the upper (+) and the lower (−) energies (interaction strength) with the PPC effect. $\tilde{\omega}_\mathrm{p}$ denotes the effective plasma frequency and is equal to $\sqrt{\omega_p^2+(n_{2D}e^2/m_\mathrm{e}|\Pi_0(\mathbf{q}_{//},\omega=0)|)}$. $V_{\mathbf{q}_{//}}$ is the 2D Coulomb interaction in Fourier domain [22]. $C(\pm)$ is the partition ratio to the upper or the lower branch of the PPC.

The 2D net plasmon–phonon generation rate in a GaAs QW is given by

$$\frac{\partial N_{i(\pm)}}{\partial t} = \frac{\sqrt{2m_{e1}^3k_BT_CA}}{\pi\hbar^4\mathrm{q}_{//}}M_{i(\pm)}^2[N_{i(\pm)}(T_C)-N_{i(\pm)}] \times\int_{\varepsilon_{\min}}^{\infty}\frac{1}{\sqrt{\varepsilon}}\left[f(\varepsilon+\varepsilon_1)-f\left(\varepsilon+\varepsilon_1+\frac{\hbar\omega_{i(\pm)}}{k_BT_C}\right)\right]\mathrm{d}\varepsilon, \tag{5}$$

where $m_{e1}$ represents the electron's effective mass in the GaAs layer. $T_C$ denotes the carrier temperature, while $k_B$ and $A$ keep their usual meanings. $N_{\mathrm{i}(\pm)}(T_C)$ and $N_{\mathrm{i}(\pm)}$ are, respectively, the Bose–Einstein number [25] at $T_C$ and the nonequilibrium phonon (plasmon) number to be determined. $f(\cdot)$ represents the electron's distribution as a function of an normalized energy to $k_BT_C$. $\varepsilon_1$ denotes the normalized ground-state energy.

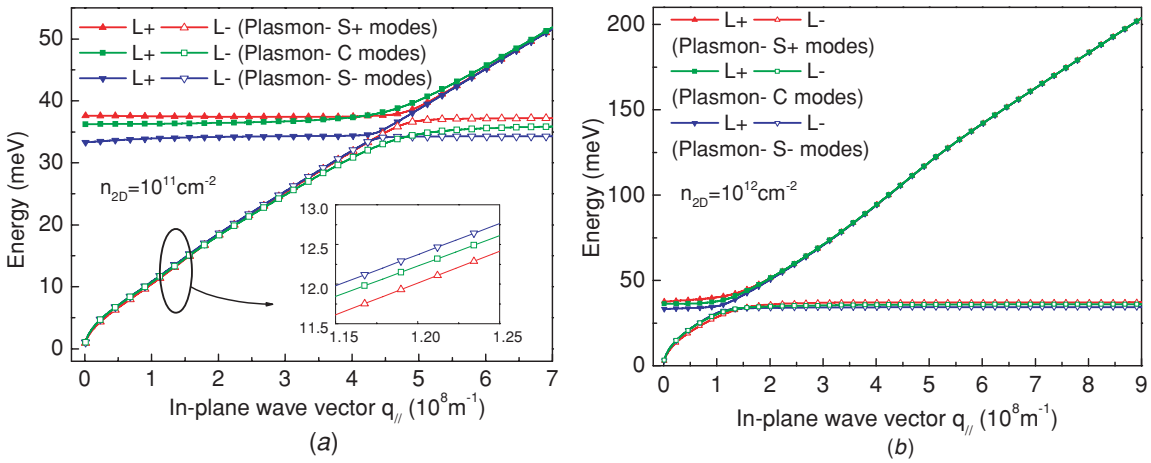


**Figure 1.** Dispersion relations of plasmon–phonon couplings in a 10 nm GaAs/$Al_{0.24}Ga_{0.76}As$ QW at sheet carrier densities of $10^{11}$ $cm^{-2}$ and $10^{12}$ $cm^{-2}$. The inset of figure 1(*a*) shows its enlarged plot of L− branches.

$\varepsilon_{\min}$ is the minimum normalized energy required for an electron to kick out plasmon–phonon coupled modes at the in-plane wave vector $\mathbf{q}_{//}$ and is given by

$$\varepsilon_{\min} = \frac{m_{e1}}{2\hbar^2 q_{//}^2 k_B T_C}\left|\frac{\hbar^2 q_{//}^2}{2m_{e1}} - \hbar\omega_{i(\pm)}\right|^2. \tag{6}$$

The net generation rate in the AlGaAs region was treated as the uncoupled case because excess electrons were simulatively generated in the well region. The hot phonon (plasmon) effect and the dynamical screening were taken into consideration. The determination of nonequilibrium phonon's (plasmon's) occupation can be obtained by solving the steady-state phonon's (plasmon's) Boltzmann equation [23]. The treatment of dynamical screening consisted in considering the 2D electronic dielectric function with the random phase approximation (RPA) into the interaction strengths [23]. The AELR is given by

$$\mathrm{AELR} = \frac{1}{n_{2D}A}\sum_{\mathbf{q}_{//},q_z,(\pm)} \hbar\omega_{i(\pm)}\frac{\partial N_{i(\pm)}}{\partial t}, \tag{7}$$

where $q_z$ denotes the quantized wave vector parallel to the crystal growth direction and is only valid for the PC mode. $q_z$ is equal to $p\pi/L$, where $p$ is a positive integer and $L$ is the well width. In our report, the fundamental mode ($p = 1$) was considered.

## Results and discussion

Our calculation was performed in a 10 nm wide GaAs/$Al_{0.24}Ga_{0.76}As$ QW. The carrier temperature of 300 K and an initial lattice temperature of 15 K were assumed. Figures 1(*a*) and (*b*) show the coupled plasmon–phonon energies as a function of the in-plane wave vector for the sheet carrier densities of $10^{11}$ and $10^{12}$ $cm^{-2}$, respectively. The PS+, the PS− and the PC coupled modes are shown in the plots, where L+ and L− represent the upper and the lower branches for each coupled mode, respectively. As the energy of the L− branch increases with an in-plane wave vector and approaches to that of the L+ branch, the two vibration modes couple with each other and the energies of the two branches split, where a plasmon bandgap (or anticrossing) is formed. The L+ and L− branches below the value of the in-plane wave vector at which the PPC take places, which will be shortened as the in-plane wave vector coupling value and denoted as $\mathbf{q}_{//c}$, behave as the phonon-like and the plasmon-like modes, respectively. Above the in-plane wave vector coupling value, the behavior is reversed so that the L+ behaves as the plasmon-like while the L− behaves as the phonon-like modes. The magnitude of plasmon bandgap of the PC, the PS+ and the PS− modes is independent of other two modes since the PPC was treated individually for each phonon mode in a QW. As the sheet carrier density increases, the in-plane wave vector coupling value decreases. Due to the conservation of energy and momentum, the exchanged in-plane wave vector between electrons and plasmon–phonon mode lies in the certain range $\left(q_{//\min} = k_{//}\left[1 - \chi_{\mathbf{k}_{//}}^{i(\pm)}\right] \leqslant q_{//} \leqslant k_{//}\left[1 + \chi_{\mathbf{k}_{//}}^{i(\pm)}\right] = q_{//\max}\right)$, where $E(\mathbf{k}_{//})$ denotes an electron's energy (in-plane wave vector) and $\chi_{\mathbf{k}_{//}}^{i(\pm)}$ is equal to $\sqrt{1 - \hbar\omega_{i(\pm)}/E(\mathbf{k}_{//})}$. As the in-plane wave vector coupling value is small enough ($q_{//c} < q_{//\min}$), the PPC does not affect the net generation rate, that is, there has been no impact on the net generation rate.

Figures 2(*a*) and (*b*) show the net plasmon–phonon generation rates as a function of the in-plane wave vector for the sheet carrier densities of $10^{11}$ and $10^{12}$ $cm^{-2}$, respectively. The generation rate of the L− branch of the PS+ mode is shown in the right axis while the rest is depicted in the left. The two cases of sheet densities have very different behavior. For the sheet density of $10^{11}$ $cm^{-2}$, since the in-plane wave vector coupling value is large, the L+ and L− branches in a certain range of wave vector ($q_{//\min} \leqslant q_{//} \leqslant q_{//\max}$) almost correspond to the phonon-like and the plasmon-like modes, respectively. In general, the low partition ratio to the L− branch shown in the inset of figure 2(*a*) leads the plasmon-like modes to contribute a minor AELR. However, the PS+ plasmon-like branch shows a much higher net generation rate than others. This is attributed to the very low energy shown in the inset of figure 1(*a*), which can result in more excitations than other modes at a given carrier temperature on the basis of the Bose–Einstein relation. The considerable net generation

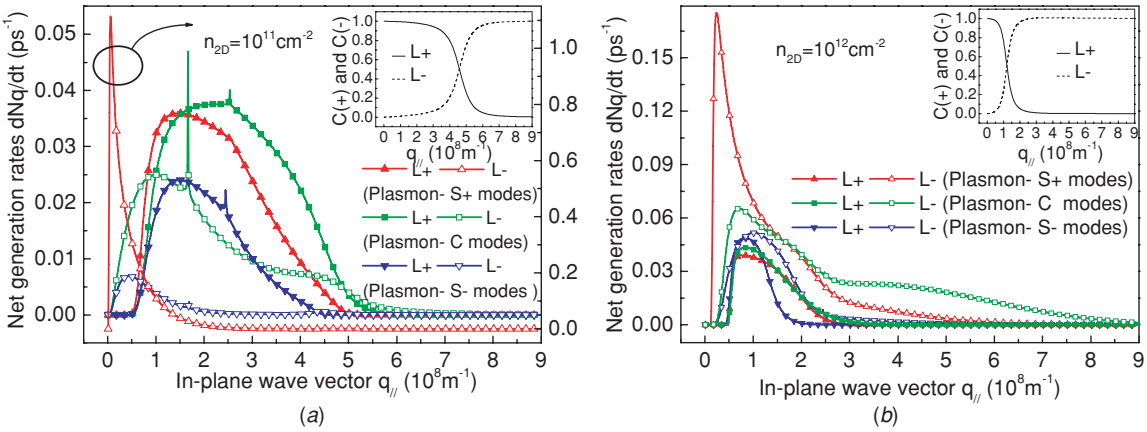


**Figure 2.** Net generation rates of plasmon–phonon couplings in a 10 nm GaAs/$Al_{0.24}Ga_{0.76}As$ QW at sheet carrier densities of $10^{11}$ cm$^{-2}$ and $10^{12}$ cm$^{-2}$. The carrier temperature of 300 K and the initial lattice temperature of 15 K were used. The hot phonon (plasmon) effect and dynamical screening were considered. Inset plots show the partition ratio of interaction strength to the plasmon and phonon as a function of an in-plane wave vector.

rate therefore enhances the AELR. The result also indicates the importance of the S+ interface phonon on the PPC. In the bulk-like phonon model where the only confined phonon in a QW is considered while the Q2D electron's wavefunction is treated accurately, a lack of S+ interface phonon mode therefore cannot anticipate the AELR enhancement due to the PPC. Otherwise, interface phonons have a stronger interaction with electrons in a QW with a well width narrower than 10 nm or an Al composition higher than 0.24 [23]. Hence, the AELR enhancement due to the PPC will be more striking in such abrupter structures.

For the sheet density of $10^{12}$ cm$^{-2}$, the in-plane wave vector coupling value is nearly $1.2 \times 10^8$ m$^{-1}$. Since the coupling value is small, which is on the left side of a certain range of in-plane wave vector ($q_{// \min} \leqslant q_{//} \leqslant q_{// \max}$), a small part of the L− branch belongs to the plasmon-like mode and its net generation rate decreases quickly as an increased wave vector because the L− branch quickly rises to the phonon's energy, where a significant reduction of PS+ net generation as compared with that in figure 2(*a*) can be found. As for the L+ branch, although a large part belongs to the plasmon-like mode, the plasmon energy is high and the excitation is low at a given carrier temperature. Hence, at the sheet density, the plasmon-like mode becomes minor to contribute the AELR. As will be seen later, the AELR enhancement due to the PPC considerably weakens.

In addition to the plasmon-like issue, there is an interesting result regarding the interface phonons. In the absence of the PPC, the S− interface phonon always has a much weaker interaction with an electron than the S+ interface and the confined phonons [23]. However, after the PPC was considered, an anomalous result was found. Around the in-plane wave vector of $10^8$ m$^{-1}$, the PS− phonon-like mode shows a slightly higher net generation rate than that of the PS+ and PC modes due to its property of lowest energy, which shows again a sensitive dependence of plasmon–phonon energy on the AELR.

In figure 2(*a*) some spikes appear in curves, which are due to the 2D Fermi's golden rule discussed below. First, the Dirac delta function $\delta[E(\mathbf{k}_{//} + \mathbf{q}_{//}) - E(\mathbf{k}_{//}) - \hbar\omega_{i(\pm)}]$ in the golden rule can be rearranged as $\delta(\hbar^2 q_{//}^2/2m_{e1} + \hbar^2 k_{//} q_{//} \cos\theta/m_{e1} - \hbar\omega_{i(\pm)})$, where $\theta$ is the angle between $\mathbf{k}_{//}$ and $\mathbf{q}_{//}$, after assuming the parabolic band structure. Then, as the net generation rate is summed over all electronic states ($\mathbf{k}_{//}$), the Dirac delta function disappears and leaves a coefficient proportional to $m_{e1}/\hbar^2 k_{//} q_{//} s$, where the $1/k_{//}$ dependence will be canceled out when the 2D density of states ($\propto k_{//}\, dk_{//}$) is substituted, giving rise to the $dE/\sqrt{E}$ dependence after an algebraic rearrangement. Thirdly, according to the momentum and energy conservation, as the electron's wave vector is larger than the value $\frac{m_{e1}}{\hbar^2 q_{//}}\left(\frac{\hbar^2 q_{//}^2}{2m_{e1}} - \hbar\omega_{i(\pm)}\right)$, a scattering to kick out the $\mathbf{q}_{//}$ phonon (plasmon) can occur. Thus, the integral range in the net generation rate has a minimum requirement as shown in equation (6). Finally, if there exists a phonon (plasmon) whose $\mathbf{q}_{//}$ satisfies $\hbar^2 q_{//}^2/2m_{e1} = \omega_{i(\pm)}$, the integration in the net generation rate passes the zero energy and the $dE/\sqrt{E}$ dependence in the integrand hence results in the spike. For those curves in figures 2(*a*) and (*b*), there is not a spike in them because their dispersion relations $\omega_{i(\pm)}$ have no phonon (plasmon) whose $\mathbf{q}_{//}$ satisfies the above condition. As compared with the nearly dispersionless relation such as the uncoupled phonon modes, the spike always appears as shown in [23].

Figure 3 shows the dependence of the AELR on the sheet carrier density, where the solid line represents the AELR with the PPC while the dash line the AELR without the PPC. Due to the PPC, the AELR is enhanced around the sheet density of $10^{11}$ cm$^{-2}$. The enhancement is due to the contribution of PS+ plasmon-like modes. As the sheet density decreases from $10^{11}$ cm$^{-2}$, the plasmon energy becomes lower and the in-plane wave vector coupling value moves to a higher value. This leads to a lower partition ratio shown in equation (4) and results in a weaker electron–plasmon scattering. On the other hand, as the sheet density increases from $10^{11}$ cm$^{-2}$, the plasmon energy increases, it is harder to excite these plasmons and thus the electron–plasmon scattering weakens.

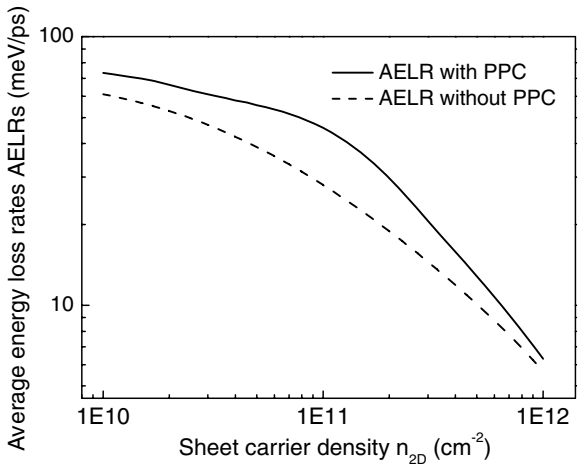


**Figure 3.** Comparison between the AELR with and without the PPC as a function of sheet density. The hot phonon (plasmon) effect and dynamical screening were considered. The carrier temperature of 300 K and the initial lattice temperature of 15 K were used.

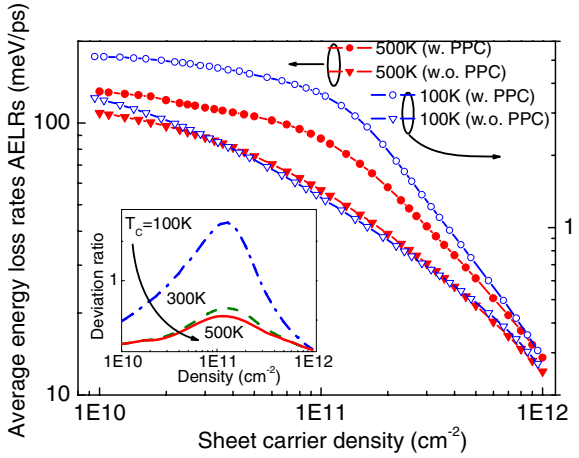


**Figure 4.** Effect of carrier temperature on the AELR with the PPC. The hot phonon (plasmon) effect and dynamical screening were considered. The initial lattice temperature of 15 K was assumed. The inset plot shows the deviation ratio of $(\mathrm{AELR_{w.PPC}} - \mathrm{AELR_{w.o.PPC}})/\mathrm{AELR_{w.o.PPC}}$ for three different carrier temperatures.

Figure 4 shows the effect of the carrier temperature on the AELR, where the left axis represents the case of 500 K while the right axis represents that of 100 K. The initial lattice temperature is at 15 K. The AELR enhancement due to the PPC was found to be stronger at 100 K than at 500 K, which is a point clearer in the inset of the deviation ratio defined as $(\mathrm{AELR_{w.PPC}} - \mathrm{AELR_{w.o.PPC}})/\mathrm{AELR_{w.o.PPC}}$. This is attributed to massive plasmons excited at a high carrier temperature causing cooling electrons to reabsorb the plasmon to recover an excited state. The so-called hot-plasmon effect thus smears the AELR enhancement. While the AELR enhancement decreases with the carrier temperature, the sheet density referred to the enhancement is insensitive to the carrier temperature.

In conclusion, plasmon–confined phonon and the plasmon–interface phonon couplings in a QW were proposed. By using the renormalized phonon propagator, the coupled dispersion and the net plasmon–phonon generation rate were obtained to calculate the AELR. Around the sheet density of $10^{11}$ cm$^{-2}$, the AELR is enhanced as compared with that without the PPC. The possibility of electron–plasmon scattering was pointed out and the importance of interface phonon modes on the PPC was also indicated. An anomalous result caused by the PPC regarding a stronger electron–S− interface phonon scattering than that of S+ interface phonon and confined phonon scatterings was also demonstrated. Finally, the hot-plasmon effect was proposed and used to explain the smearing AELR enhancement as the carrier temperature increases.

## Acknowledgment

We acknowledge the support from National Science Council under grant no NSC 91-2120-E009-003.

## References

[1] Mishchenko E G, Reizer M Yu and Glazman L I 2004 *Phys. Rev.* B **69** 195302
[2] Aizin G R, Laikhtman B and Gumbs G 2001 *Phys. Rev.* B **64** 125317
[3] Wang X F 2005 *Phys. Rev.* B **72** 085317
[4] Ullrich C A and Vignale G 2001 *Phys. Rev. Lett.* **87** 037402
[5] Cheng S J and Gerhardts R R 2001 *Phys. Rev.* B **63** 035314
[6] Liu X H, Wang X H and Gu B Y 2001 *Phys. Rev.* B **64** 195322
[7] Tselis A C and Quinn J J 1984 *Phys. Rev.* B **29** 3318
Sarma S D and Quinn J J 1982 *Phys. Rev.* B **25** 7603
[8] Finck A D K, Champagne A R, Eisenstein J P, Pfeiffer L and West K W 2008 *Phys. Rev.* B **78** 075302
[9] Armitage A, Andrews S R, Cluff J A, Huggard P G, Linfield E H and Ritchie D A 2004 *Phys. Rev.* B **69** 125309
[10] Bootsmann M-T, Hu C-M, Heyn C H, Heitmann D and Schüller C 2003 *Phys. Rev.* B **67** 121309(R)
[11] Hirjibehedin C F, Pinczuk A, Dennis B S, Pfeiffer L N and West K W 2002 *Phys. Rev.* B **65** 161309
[12] Fasol G, King-Smith R D, Richards D, Ekenberg U, Mestres N and Ploog K 1989 *Phys. Rev.* B **39** 12695
Merlin R, Bajema K, Clarke R, Juang F-Y and Bhattacharya P K 1985 *Phys. Rev. Lett.* **55** 1768
[13] Hwang E H and Sarma S D 2001 *Phys. Rev.* B **63** 233201
Mahan G D 2000 *Many-Particle Physics* (New York: Kluwer/Plenum)
[14] Aguado R, Lopez-Sancho M P, Sinova J and Brey L 2004 *Phys. Rev.* B **70** 195201
[15] Klimin S N, Fomin V M and Devreese J T 2008 *Phys. Rev.* B **77** 205311
[16] Venger E F and Piskovoi V N 2004 *Phys. Rev.* **70** 115107
[17] Yee K J, Yee D S, Kim D S, Dekorsy T, Cho G C and Lim Y S 1999 *Phys. Rev.* B **60** R8513
[18] Sapega V F, Chamberlain M P, Ruf T, Cardona M, Mirlin D N, Tötemeyer K, Fischer A and Eberl K 1995 *Phys. Rev.* B **52** 14144
[19] Jain J K, Jalabert R and Sarma S D 1988 *Phys. Rev. Lett.* **60** 353
Sarma S D, Jain J K and Jalabert R 1988 *Phys. Rev.* B **37** 6290
[20] Wendler L and Pechstedt R 1987 *Phys. Rev.* B **35** 5887
[21] Mori N and Ando T 1989 *Phys. Rev.* B **40** 6175
[22] Lee H C, Sun K W and Lee C P 2002 *J. Appl. Phys.* **92** 268
[23] Lee H C, Sun K W and Lee C P 2003 *Solid State Commun.* **128** 245–50
[24] Adachi S 1985 *J. Appl. Phys.* **58** R1
[25] Devreese J T and Peeters F M 1987 *The Physics of the Two-Dimensional Electron Gas* (New York: Plenum) pp 183–225